Journal of Thermal Analysis, Vol. 30 (1985) 83–96

DETERMINATION OF THE KINETICS AND MECHANISM OF THERMAL DEHYDRATION OF SOME URANYL CARBOXYLATE COMPOUNDS BY ISOTHERMAL AND NON-ISOTHERMAL PROCEDURES

*R. M. Rojas, M. L. de Paz** and *E. Vila*

INSTITUTO Q. INORGÁNICA "ELHUYAR" C. S. I. C., SERRANO 113, MADRID 6;
* DEPARTAMENTO Q. INORGÁNICA, F. DE QUIMICAS, U. COMPLUTENSE,
MADRID 3, SPAIN

The kinetics and mechanism of the thermal dehydration of uranyl *trans*-hexenedioate monohydrate $[UO_2(C_6H_6O_4) \cdot H_2O]$ and uranyl fumarate $[UO_2(C_4H_2O_4) \cdot H_2O]$ have been studied by means of isothermal and non-isothermal gravimetric methods. The rate equations that provide the most accurate fit to the experimental data were determined by the usual procedures and with a computer program that allows almost quantitative comparison of each set of experimental (α, t) values with any rate equation $F(\alpha)$. For the experimental data obtained at linearly increasing temperatures the Coats and Redfern equation was used, but assuming that the functions estimated by means of the isothermal method are also valid for the non-isothermal runs. The kinetics parameters derived from the dynamic TG method show clear dependences on the heating rate and particle size, but they are related by the compensation law.

The thermal dehydration and decomposition of some metal carboxylate compounds have been studied in great detail, and in some cases the results obtained from the thermal data have been related with their crystal structures [1–3].

In this paper we study the kinetics of thermal dehydration of uranyl *trans*-hexenedioate monohydrate and uranyl fumarate monohydrate by means of both isothermal and non-isothermal procedures; the data obtained under different conditions are analyzed and compared with those obtained from the isothermal runs.

Experimental

Sample preparation

Uranyl *trans*-hexenedioate monohydrate was obtained from a very dilute aqueous solution of *trans*-hexenedioic acid, rubidium hydroxide and uranyl nitrate hexahydrate in the molar ratio 2:1:2. After a short standing, very small crystals appeared; they could not be recrystallized because of the low solubility in the most common solvents.

John Wiley & Sons, Limited, Chichester
Akadémiai Kiadó, Budapest

Uranyl fumarate monohydrate precipitated as a deep-greenish yellow powder on the addition to a solution of uranyl nitrate hexahydrate of a warm solution of fumaric acid and sodium hydroxide in the molar ratio 1:1:2 [4]. The addition order has to be kept, as otherwise a sodium uranyl fumarate derivative is formed.

The quantitative analyses of these compounds were as follows:

Calculated for $[UO_2(C_6H_6O_4) \cdot H_2O]$: %C 16.74; %H 1.86; %U 55.34.
Found: %C 16.75; %H 2.01; %U 55.85.
Calculated for $[UO_2(C_4H_2O_4) \cdot H_2O]$: %C 11.94; %H 0.99; %U 59.20.
Found: %C 12.88; %H 1.08; %U 59.17.

The X-ray powder data for these compounds and anhydrous uranyl fumarate are listed in Table 1. The X-ray powder diagram of anhydrous uranyl *trans*-hexenedioate shows only very poorly defined lines.

Table 1 X-ray powder data for uranyl fumarate monohydrate, anhydrous uranyl fumarate and uranyl *trans*-hexenedioate monohydrate

$[UO_2(C_4H_2O_4) \cdot H_2O]$		$[UO_2(C_4H_2O_4)]$		$[UO_2(C_6H_6O_4) \cdot H_2O]$	
d, Å	I/I_0	*d*, Å	I/I_0	*d*, Å	I/I_0
6.00	70	6.14	50	6.48	30
5.16	100	5.19	30	5.97	60
5.04	65	4.88	15	5.44	10
4.73	10	4.20	20	5.09	10
4.28	50	4.00	100	4.41	100
3.90	40	3.78	15	4.21	15
3.87	90	3.53	10	4.05	50
3.09	30	3.40	20	3.68	10
2.94	20	3.13	10	3.52	10
2.90	45	2.81	10	3.44	40
2.82	45	2.64	15	3.25	10
2.75	15	2.44	15	3.00	20
2.53	10			2.92	10
2.52	15			2.86	20
2.37	5			2.65	30
2.33	15			2.63	15
2.31	5			2.54	30
2.25	40			2.41	30
2.22	10			2.34	10
2.15	5				
2.13	10				

Thermoanalytical methods

The dynamic TG and DTA curves of the two compounds in the temperature range 298–973 K are shown in Fig. 1. It can be seen that dehydration occurs at relatively high temperatures; this may be indicative of the coordination of the water molecules to the uranyl ion, but this assumption is not supported by any additional evidence,

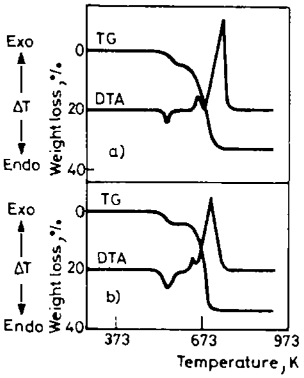

Fig. 1 DTA and TG curves of a) uranyl fumarate monohydrate, b) uranyl *trans*-hexenedioate monohydrate

Table 2 Temperatures and heating rates used for the isothermal and non-isothermal dehydration of the uranyl carboxylates

Compound	Isothermal studies T, K	Non-isothermal studies Heating rates, deg/min^{-1}
$[UO_2(C_6H_6O_4) \cdot H_2O]$ crystals	508, 513, 518 523, 528	5, 10, 20
$[UO_2(C_6H_6O_4) \cdot H_2O]$ powder	503, 508, 513 518, 523	5, 10, 20
$[UO_2(C_4H_2O_4) \cdot H_2O]$ powder	503, 508, 513 518, 523	5, 10, 20

since the crystal structures of these compounds have not yet been resolved and their i.r. spectra do not provide enough information.

Kinetic methods

The isothermal runs were performed in static air atmosphere, using a 951 Dupont Thermogravimetric Analyzer coupled with a 990 Thermal Analyzer, at the temperatures indicated in Table 2. Powdered samples which passed through a 200 mesh sieve (0.074 mm internal diameter) were used for both compounds, and crystals of uranyl *trans*-hexenedioate monohydrate were also studied without being subject to initial grinding. About 8 mg sample was weighed in each run.

The dynamic TG traces obtained at different heating rates (Table 2) were recorded under otherwise identical conditions.

The DSC measurements were made with a Dupont DSC cell at 10 deg/min^{-1}; temperature and enthalpy change were calibrated via the melting point of tin at 504.9 K with ΔH = 14.14 mcal/mg.

Microscopic observations

Microscopic examination of uranyl *trans*-hexenedioate monohydrate crystals during dehydration was made with a Karl Zaner Wetzlar microscope having a hot-stage attachment.

Photographs were taken on crystals directly heated on the hot-stage at about 20 deg/min^{-1}, and on crystals placed on the stage previously heated and held at 513 K; in this case pictures of the crystals were taken every 8–10 s. Photographs were also taken of crystals isothermally heated in the thermobalance at 508 K for different periods of time.

Results and discussion

Isothermal studies

a. *Uranyl trans-hexenedioate monohydrate crystals*

The experimental α (fraction reacted) obtained at the temperatures indicated in Table 2 were plotted against $t/t_{0.5}$ and $t/t_{0.9}$; the ln ln approximation [5] indicates that the reaction is isokinetic in the temperature range considered (Fig. 2). From these two methods it can be estimated that a second-order Avrami–Erofe'ev equation fits the experimental data very well, and the Jones approach [6] leads to the same conclusions. In Fig. 3a, the plot of $(t/t_{0.5})_{\text{exp.}}$ vs $(t/t_{0.5})_m$ for common values of $\alpha_{\text{exp.}}$ and α_m is a straight line of unit slope through the origin, indicating that the selected rate equation is obeyed; similarly, the plots of $t_{\text{exp.}}$ vs $(t/t_{0.5})_m$ are straight lines with slopes $(t_{0.5})_{\text{exp.}}$ passing through the origin.

Nevertheless, the above methods of identification of the rate equations can be shortened by using a computer program. A program that allows quantitative com-

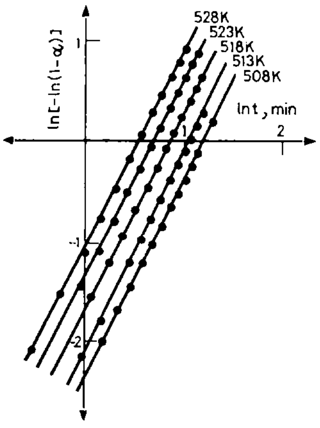

Fig. 2 Plot of $-\ln\ln(1-\alpha)$ vs. ln time for the dehydration of $[UO_2(C_6H_6O_4)\cdot H_2O]$ crystals

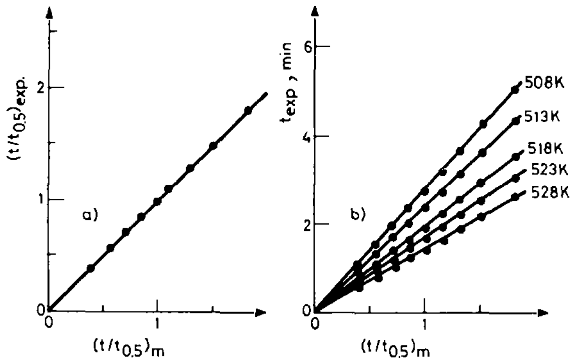

Fig. 3 Reduced time plots obtained by application of the Jones method to the dehydration of uranyl *trans*-hexenedioate monohydrate crystals

parison between any rate equation and each set of experimental (α, t) values obtained at any temperature has been used.*

It is well known that rate equations can be expressed in the form $F(\alpha) = kt$; by plotting against time the $F(\alpha)$ values obtained at every temperature, the rate equation that best describes the mechanism of dehydration can be searched for. This will generate a straight line of slope k (rate constant) passing through the origin.

Table 3 lists the correlation coefficients (r) and errors (δ) calculated for the least squares fitting of the $F(\alpha)$ vs. time plot for the (α, t) values obtained at 508 K. On the basis of these two criteria (r and δ), the equations R_1, A_2 and R_2 could describe the dehydration process. The question arises as to how to choose between them. At this point it is worth bearing in mind that the criteria based on the absolute error concepts are not sufficient and can lead to errors, since they do not consider the range in which the $F(\alpha)$ values lie, this being different for each rate equation (Fig. 4). Some additional criteria based on the relative concepts, that do take into account the $F(\alpha)$ range, have been introduced. The mean relative error ($\bar{Er}$) and its associated standard deviation (S) are considered, where

$$\bar{Er} = \frac{\sum_i |Er_i|}{N}, \quad S = \left[\frac{\sum_i (|Er_i| - \bar{Er})^2}{N-1}\right]^{\frac{1}{2}}$$

and N = number of experimental data.

When the correct $F(\alpha)$ is used, its plot vs. time will be a straight line through the origin, the intercept with the y axis (C_0) being zero).

Table 3 shows the $\bar{Er}$, S and C_0 values calculated for the various equations and temperature, together with the correlation coefficients (r) and errors (δ). Figure 4 reproduces the plots of $F(\alpha)$ vs. time for the (α, t) obtained at 508 K for this compound; the best agreement over the whole temperature range is observed for the equation A_2.

---

* This program, written in BASIC, is available on request from the authors.

Table 3 Relative errors, standard deviation and *y*-intercept calculated for isothermal dehydration of uranyl *trans*-hexenedioate crystals. (The symbols of Hancock and Sharp have been used)

		$F(\alpha)$									
T, K		D_1	D_2	D_3	D_4	F_1	R_2	R_3	R_1	A_2	A_3
508	r	0.9708	0.9577	0.9396	0.9510	0.9885	1.0000	0.9943	0.9994	0.9992	0.9958
	$\delta \times 10^3$	36.871	29.725	10.935	7.848	53.251	11.269	10.346	6.836	6.902	18.883
508	$\bar{E}r$	226.56	330.04	491.35	377.97	23.29	11.95	14.87	3.65	0.54	2.45
	S	632.5	919.68	1370.57	1053.10	44.62	23.63	29.18	8.52	0.41	2.57
	C_0	−0.20	−0.14	-4.34×10^{-2}	-3.43×10^{-2}	−0.35	−0.11	8.9×10^{-2}	−0.15	8.00×10^{-3}	0.23
513	$\bar{E}r$	183.58	332.19	641.52	416.93	32.22	10.32	16.19	3.72	0.26	2.42
	S	562.27	1013.61	1936.76	1265.54	66.83	22.54	34.21	2.76	0.25	2.75
	C_0	−0.29	−0.23	9.17×10^{-2}	-6.28×10^{-2}	−5.8	−0.15	−0.12	−0.14	-7.7×10^{-3}	0.25
518	$\bar{E}r$	119.02	256.78	508.74	343.09	33.51	7.72	13.47	8.21	0.78	2.56
	S	365.60	770.84	1752.43	1024.78	70.38	16.67	30.13	7.72	0.47	2.66
	C_0	−0.30	−0.27	−0.12	-7.6×10^{-2}	−0.69	−0.15	−0.13	−0.10	2.09×10^{-3}	0.28
523	$\bar{E}r$	534.27	1208.89	3179.02	1682.23	90.13	20.88	36.02	13.31	0.62	3.44
	S	1921.72	4283.41	1115.13	5935.99	236.52	55.33	97.45	14.88	0.40	2.59
	C_0	−0.25	−0.25	−0.13	-7.3×10^{-2}	−0.73	−0.13	−0.12	-6.63×10^{-2}	-1.33×10^{-4}	0.27
528	$\bar{E}r$	256.04	592.61	1731.06	860.53	71.80	13.51	24.77	14.49	0.61	3.05
	S	814.96	1950.61	5596.74	2807.43	172.84	31.28	63.23	18.36	0.47	3.55
	C_0	−0.25	−0.26	−0.15	-7.9×10^{-2}	−0.81	−0.13	−0.13	-4.5×10^{-2}	7.2×10^{-3}	0.29

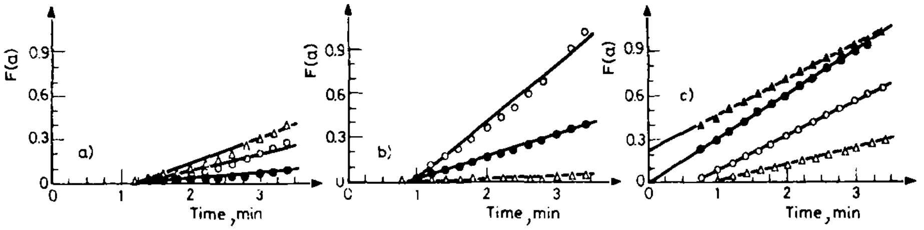

Fig. 4 Plots of $F(\alpha)$ vs. time for the dehydration of $[UO_2(C_6H_6O_4) \cdot H_2O]$ crystals, and their regression lines at 508 K (the symbols are those of Hancock and Sharp). a: △ D_1, ○ D_2, ● D_3; b: △ D_4, ○ F_1, ● R_2; c: △ R_3, ○ R_1, ● A_2, ▲ A_3

b. *Uranyl trans-hexenedioate monohydrate powdered samples*

Crystals of this compound were ground and the fraction passing through a 200 mesh sieve was used.

In this case, the reduced time plots (Fig. 5) indicate that the experimental data fit the Avrami–Erofe'ev equation $[-\ln(1-\alpha)]^{1/2} = kt$ up to an α value of 0.7, while for $0.7 < \alpha < 0.9$ they better fit the master curve obtained for an F_1 equation [7]; computer calculations led to the same results.

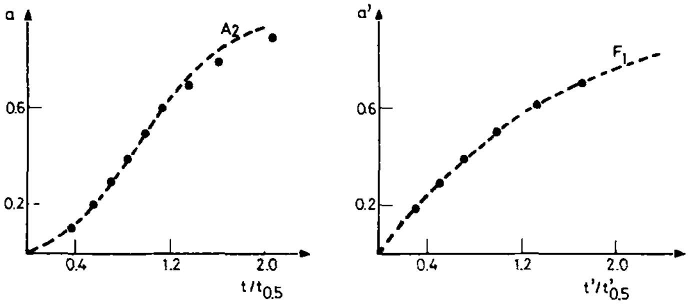

Fig. 5 Reduced time plots for the dehydration of powdered uranyl *trans*-hexenedioate monohydrate; — — — master curve, ● experimental values $\alpha' = \frac{\alpha - 0.7}{1 - 0.7}$, $t' = t - t_{0.7}$

c. *Uranyl fumarate monohydrate*

This compound was obtained as a microcrystalline powder, and the fraction passing through a 200 mesh sieve was used.

The rate equation that best fitted the experimental (α, t) data obtained at various constant temperatures was determined as described above, and corresponded to a second-order Avrami–Erofe'ev equation.

The rate constants at various temperatures, the activation energies and pre-exponential factors derived from the Arrhenius plots, and the enthalpy changes obtained for the dehydration reactions studied here are given in Table 4.

Non-isothermal methods

With these methods, the reaction kinetics can be studied from a single curve, this being the main advantage of the procedure; nevertheless, the results obtained are not very consistent, since under dynamic conditions the mechanism of the reaction depends on numerous physico-chemical factors and experimental conditions. Very low heating rates are usually used in the hope that these better reproduce the isothermal conditions. However, as shown below, the discrepancy between the values of the kinetic parameters obtained with the two methods is considerably higher when lower heating rates are used.

In the analysis of the dynamic TG curves obtained at linearly increasing temperatures, the Coats and Redfern equation has been used; it has been assumed that the function $F(\alpha)$ obeyed isothermally is also valid for the non-isothermal runs over all the heating programs used [8–11]:

$$\ln\frac{F(\alpha)}{T^2} = \ln\frac{AR}{\beta E}\left(1-\frac{2RT}{E}\right)-\frac{E}{RT} \tag{1}$$

where the symbols have the usual meaning and β is the linear heating rate.

The kinetic parameters obtained for each compound are listed in Table 6, with the heating rates used and the temperatures of inception and completion of the dehydration reactions; the latter increase as the heating rate does, but the opposite trend is observed in the activation energies and in the values of the pre-exponential factor.

When the equation proposed by Flor [8] was used to check the above assumption, the agreement between the experimental and calculated (α, t) was quite poor, but it improved at higher heating rates, and the E_a and A values obtained under these conditions almost agreed with those determined with the isothermal procedures. All the other rate equations commonly used were also tested, but no agreement between the experimental and calculated (α, t) could be attained. At this point we have to consider the possibility that a single rate equation cannot account for the dehydration process under non-isothermal conditions.

In spite of the disparity of the values obtained for the activation energy and the pre-exponential factor, they seem to be related by the compensation effect [12, 13] according to the relation $\ln A = a + bE$.

The T_{critical} values for the reactions studied here were calculated via the expression

$$\frac{1}{T_{\mathrm{cr}}} = \frac{1}{T_{\mathrm{max}}} + \frac{R}{E}\ln\frac{E\beta}{RT_{\mathrm{max}}^2} \tag{2}$$

where T_{max} is the temperature for $\mathrm{d}\alpha/\mathrm{d}t$ maximum.

Table 4 Rate constants, activation energies, pre-exponential factors and enthalpy changes obtained for the dehydration of the uranyl carboxylate compounds

Compound								
$[UO_2(C_6H_6O_4)\cdot H_2O]$ crystals		$[UO_2(C_6H_6O_4)\cdot H_2O]$ powder					$[UO_2(C_4H_2O_4)\cdot H_2O]$ powder	
T, K	$k\cdot 10^3$, sec^{-1}	T, K	$k\cdot 10^3$, sec^{-1}	α range	α range	$k\cdot 10^3$, sec^{-1}	T, K	$k\cdot 10^3$ sec^{-1}
508	4.9183	503	3.9216	0.14–0.71	0.71–0.92	7.670	503	2.615
513	5.8016	508	4.6583	0.12–0.70	0.71–0.93	9.330	508	3.805
518	7.0066	513	5.7966	0.06–0.71	0.72–0.92	11.196	513	5.225
523	8.1833	518	6.8333	0.05–0.71	0.71–0.95	14.360	518	7.091
528	9.5750	523	8.3366	0.05–0.73	0.74–0.94	17.118	523	9.413
$E_a = 74.73$ kJ · mol^{-1}		$E_a = 82.67$ kJ · mol^{-1}			$E_a = 88.99$ kJ · mol^{-1}		$E_a = 139.28$ kJ · mol^{-1}	
$A = 2.38 \times 10^5$ sec^{-1}		$A = 1.49 \times 10^6$ sec^{-1}			$A = 1.32 \times 10^7$ sec^{-1}		$A = 7.76 \times 10^{11}$ sec^{-1}	
$\Delta H = 74.89$ kJ · mol^{-1}				$\Delta H = 79.99$ kJ · mol^{-1}			$\Delta H = 61.76$ kJ · mol^{-1}	

Table 5 Relative errors, standard deviation and y-intercept for isothermal dehydration of powdered uranyl *trans*-hexenedioate monohydrate at 513 K

T, K	α range		$F(\alpha)$									
			D_1	D_2	D_3	D_4	F_1	R_2	R_3	R_1	A_2	A_3
513	0.1–07	$\bar{E}r$	19.08	27.31	39.67	30.94	5.89	2.93	3.81	1.11	0.33	1.87
		S	29.97	44.83	66.87	51.59	6.11	2.87	3.79	1.27	0.39	1.50
		C_0	-0.28	-0.19	-6.02×10^{-2}	-4.82×10^{-2}	-0.46	-0.15	-0.12	-0.19	4.06×10^{-3}	0.26
513	0.7–0.9	$\bar{E}r$	89.66	238.92	540.80	311.94	1.71	11.63	7.76	19.36	7.85	6.44
		S	355.17	941.66	2144.75	1250.52	2.07	28.44	18.56	46.28	14.85	9.78
		C_0	-5.83×10^{-2}	-6.65×10^{-2}	-3.16×10^{-2}	-1.94×10^{-2}	-2.78×10^{-4}	5.07×10^{-2}	2.5×10^{-2}	0.15	0.39	0.53

Table 6 Activation energies and pre-exponential factors obtained for the dehydration of the uranyl carboxylate compounds under non-isothermal conditions

Compounds	Heating rates, K · min^{-1}	Dehydration temperatures T_0, K	Dehydration temperatures T_f, K	E_a, kJ · mol^{-1}	A, sec^{-1}	$F(\alpha)$
$[UO_2(C_6H_6O_4) \cdot H_2O]$ crystals	20	519	570	93.34	$8.16 \cdot 10^6$	A_2
	10	509	563	105.27	$1.13 \cdot 10^8$	
	5	508	543	131.25	$4.98 \cdot 10^{10}$	
$[UO_2(C_6H_6O_4) \cdot H_2O]$ powder	20	505	546	84.47	$8.90 \cdot 10^7$	A_2
	10	510	545	112.76	$6.65 \cdot 10^8$	
	5	505	531	164.43	$9.90 \cdot 10^{13}$	
$[UO_2(C_6H_6O_4) \cdot H_2O]$ powder	20	546	571	142.01	$8.62 \cdot 10^{11}$	F_1
	10	545	573	166.18	$1.59 \cdot 10^{14}$	
	5	531	553	244.30	$1.18 \cdot 10^{22}$	
$[UO_2(C_4H_2O_4) \cdot H_2O]$ powder	20	521	569	126.65	$1.82 \cdot 10^{10}$	A_2
	10	501	559	143.81	$1.12 \cdot 10^{11}$	
	5	493	549	142.26	$5.28 \cdot 10^{11}$	

Table 7 Compensation relationships for dehydration of the uranyl carboxylate compounds under non-isothermal conditions

	Heating rate deg · min^{-1}	T_{max}, K	T_{cr}, K	k
$[UO_2(C_6H_6O_4) \cdot H_2O]$ crystals	20	548	555.9	0.95
	10	533.4	552.2	0.97
	5	523.7	546.3	1.01
	$\ln A = 0.96\,E_a - 1.43$			
$[UO_2(C_6H_6O_4) \cdot H_2O]$ powder	20	538.5	547.8	0.93
	10	535	550.7	0.96
	5	526	541	1.00
	$\ln A = 0.94\,E_a - 0.84$			
$[UO_2(C_4H_2O_4) \cdot H_2O]$ powder	20	546	546.6	0.96
	10	535	545.2	1.00
	5	527	546.8	1.01
	$\ln A = 0.90\,E_a - 0.38$			

The sufficiently close values obtained for T_{cr} support the view that a compensation relationship exists. In Table 7, the T_{cr} and T_{max} obtained at several heating rates have been listed and the relations obtained for each process are also indicated.

Microscopic observations

Photomicrographs of two different crystals of uranyl *trans*-hexenedioate monohydrate, heated isothermally or dynamically, are shown in Fig. 6.

When dehydration starts, the edges of the crystals become opaque (dark zones in the photographs) and identical behaviour is observed under the different conditions (Fig. 6b, e). When the reaction proceeds under non-isothermal conditions, many cracks appear on the crystal face directly observed under the microscope (Fig. 6f). They are not sites of emergent dislocations, since they penetrate into the bulk and increase in number as the reaction proceeds.

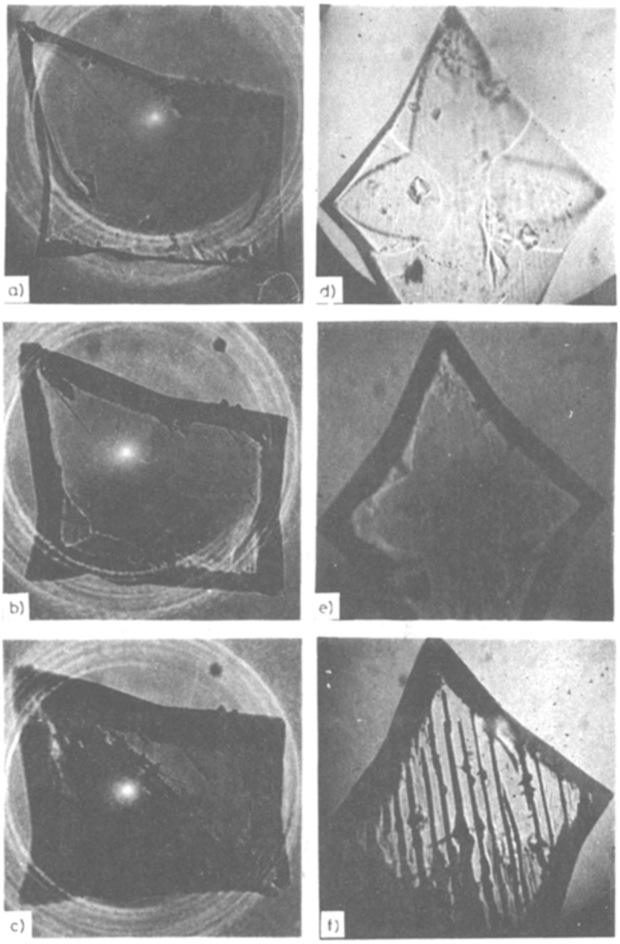

Fig. 6 Sequence of photomicrographs of two crystals of $(UO_2(C_6H_6O_4) \cdot H_2O)$; a) room temperature, b, c) 513 K, 20-minute interval between them, d) room temperature, e) 523 K, f) 553 K; heating rate: about 20 deg • min^{-1}

When the temperature is held at 513 K, some small scratches are also observed, but the interface advance occurs predominantly from the edges of the crystal inwards.

These two different types of behaviour suggest that when the dehydration takes place under non-isothermal conditions, a new mechanism overlaps with the interface advance from the edges inwards.

The existence of this new mechanism, that is not considered when the second-order Avrami–Erofe'ev equation is assumed to hold over the entire non-isothermal runs, could explain the disagreement observed between the kinetic parameters obtained with the two methods.

References

1 W. E. Brown, D. Dollimore and A. K. Galwey, in Comprehensive Chemical Kinetics, Ed. C. H. Bamford and C. F. H. Tipper, Elsevier, Amsterdam, 1980, vol. 22, and references therein.

2 C. Eckhardt and T. B. Flanagan, Trans. Faraday Soc., 60 (1964) 1289.

3 P. M. Fichte and T. B. Flanagan, Trans. Faraday Soc., 67 (1971) 2.

4 A. Müller, Z. Anorg. Chem., 109 (1920) 235.

5 J. D. Hancock and J. H. Sharp, J. Am. Ceram. Soc., 55 (1972) 74.

6 L. F. Jones, D. Dollimore and T. Nicklin, Thermochim. Acta, 13 (1975) 240.

7 J. H. Sharp, G. W. Brindley and B. N. Narahan Achar, J. Am. Ceram. Soc., 47 (1966) 379.

8 G. Flor, A. Marini and V. Berberini, Z. Naturforsch., Teil A., 34 (1979) 437.

9 H. Tanaka, Thermochim. Acta, 46 (1981) 139.

10 J. M. Criado and J. Morales, Thermochim. Acta, 19 (1977) 305.

11 T. A. Clarke and J. M. Thomas, Nature London, 219 (1968) 1169.

12 A. V. Nikolaev, V. A. Logvinenko and V. M. Gorbatchev, J. Thermal Anal., 6 (1974) 473.

13 V. M. Gorbatchev, J. Thermal Anal., 8 (1975) 585.

Zusammenfassung — Kinetik und Mechanismus der thermischen Dehydratisierung von Uranyl-trans-hexendioat-Monohydrat $[UO_2(C_6H_6O_4) \cdot H_2O]$ und Uranylfumarat $[UO_2(C_4H_2O_4) \cdot H_2O]$ wurden mittels isothermer und nicht-isothermer gravimetrischer Methoden untersucht. Die die experimentellen Werte am genauesten beschreibenden Geschwindigkeitsgleichungen wurden durch übliche Methoden und mit Hilfe eines Computerprogramms bestimmt, das einen nahezu quantitativen Vergleich aller Versuchsdatenreihen (α, t) mit jeder Geschwindigkeitsgleichung $F(\alpha)$ ermöglicht. Zur Auswertung der bei linearer Aufheizgeschwindigkeit erhaltenen experimentellen Daten wurde die Gleichung von Coats und Redfern unter der Annahme benutzt, daß die durch isotherme Methoden bestimmten Funktionen auch für nicht-isotherme Versuche gültig sind. Die durch dynamische TG erhaltenen kinetischen Parameter sind von der Aufheizgeschwindigkeit und der Teilchengröße abhängig.

Резюме — С помощью изотермических и неизотермических гравиметрических методов изучена кинетика и механизм термической дегидратации моногидратов солей уранила с фумаровой $[UO_2(C_4H_2O_4) \cdot H_2O]$ и транс-гексендикарбоновой кислотой $[UO_2(C_6H_6O_4) \cdot H_2O]$. Уравнения скорости реакций, наиболее точно соответствующих экспериментальным данным, были определены обычными методами и с помощью программы на ЭВМ, что позволило провести почти количественное сравнение каждого набора экспериментальных значений (α, t) с каким-либо уравнением скорости реакции $F(\alpha)$. Для экспериментальных данных, полученных при линейно-увеличивающихся температурах, было использовано уравнение Коутса и Рэдферна, но предполагая при этом, что полученные изотермическим методом функциональные зависимости, справедливы также и для неизотермических процессов. Кинетические параметры, установленные на основе динамической ТГ, показали четко выраженную зависимость от скорости нагрева и размера частиц.